Protein Aggregation

International Edition: DOI: 10.1002/anie.201605151
German Edition: DOI: 10.1002/ange.201605151

Gold-Induced Fibril Growth: The Mechanism of Surface-Facilitated Amyloid Aggregation

Anika Gladytz, Bernd Abel, and Herre Jelger Risselada**

Abstract: *The question of how amyloid fibril formation is influenced by surfaces is crucial for a detailed understanding of the process in vivo. We applied a combination of kinetic experiments and molecular dynamics simulations to elucidate how (model) surfaces influence fibril formation of the amyloid-forming sequences of prion protein SUP35 and human islet amyloid polypeptide. The kinetic data suggest that structural reorganization of the initial peptide corona around colloidal gold nanoparticles is the rate-limiting step. The molecular dynamics simulations reveal that partial physisorption to the surface results in the formation of aligned monolayers, which stimulate the formation of parallel, critical oligomers. The general mechanism implies that the competition between the underlying peptide–peptide and peptide–surface interactions must strike a balance to accelerate fibril formation.*

While invisible for the naked eye, nanoparticles (NPs) are all around us. Nowadays, they enter our body through the products that we use, the food that we eat, or the air that we breathe (aerosols). Whether this is associated with potential health risks is a subject of increasing interest. For example, the influence of metal NPs on the fibrillation of amyloid peptides has been intensely discussed in the literature.[1,2] The observed effects of different NPs on amyloid peptides and proteins (which are responsible for Alzheimer's and Parkinson's disease and diabetes II, for example) reach from strong acceleration of fibril formation to inhibition of peptide aggregation and destruction of preformed fibrils (for a comprehensive overview of the literature, see the Supporting Information, Table S5). Different models have been proposed to explain fibril formation in both free solution and near surfaces: The "nucleated conformational conversion" model postulates that in free solution, peptides first assemble into loose and unstructured oligomers, which are then converted into ordered β-sheet-rich fibrils in a second, rate-limiting step.[3] The condensation–ordering model assumes that in the presence of NPs, surface attractions result in an increase in the local peptide concentration and subsequently facilitate a secondary ordering step.[4] Mahmoudi et al. found that NPs alter the secondary structures of peptides and proteins[5] and therefore proposed the "surface-assisted nucleation" model.[6] The groups of Vachá and Radic independently stressed that the strength of the interaction between a peptide and a surface determines whether and how fibril formation is influenced.[7] However, none of these models explains in detail how and why the rate-limiting conversion or ordering step of unstructured oligomers (whose formation is facilitated by the condensation effect at the surface) into β-sheet-rich fibrils is influenced by surfaces.

We recently studied the kinetics of the fibril formation of the amyloid-forming sequences of human islet amyloid polypeptide (hIAPP), NNFGAIL, and the prion protein SUP35, GNNQQNY, in the presence of negatively charged citrate-stabilized gold NPs using an in vitro setup (see Figure 1).[2] The gold NPs markedly accelerated fibril growth, and they reduced the characteristic lag time from about 50 min (in a control experiment in the absence of NPs) to 15 min (for details, see Figure S14, Tables S3 and S4, and Ref. [2]). These fibrils were markedly larger and thicker than the fibrils incubated in the absence of NPs. A corona was nearly instantaneously formed around the metal NPs (see Figure 2 B).[2] To determine whether the observed corona affects the kinetics of fibril formation, we incubated NPs at a peptide concentration that is a) low enough to suppress fibril formation and b) high enough to enable corona formation. Fibril formation was initiated by a sudden increase in peptide concentration after different incubation times t_1. Fibrils became detectable at a time t_2. This time was compared to the normal lag time t_0 (non-diluted peptide solutions in the presence of NPs). Intriguingly, we found that whenever the incubation time t_1 exceeded the lag time of the system (t_0), fibril formation started instantaneously. On the other hand, in the absence of NPs, the detection time t_2 (ca. 50 min) was completely independent of the incubation time t_1 (see Table S4 and Figure S16). Thus, the rate-determining step of fibril formation in the vicinity of the gold surface is a "(re)structuring process" within the peptide corona. The restructured corona acts as a seed for fibril formation (see Figure 1).

[*] A. Gladytz, Prof. Dr. B. Abel, Dr. H. J. Risselada
Chemistry Department
Leibniz Institute of Surface Modification (IOM) Leipzig e.V.
Permoserstrasse 15, 04318 Leipzig (Germany)
E-mail: bernd.abel@iom-leipzig.de
hrissel@gwdg.de

A. Gladytz, Prof. Dr. B. Abel
Faculty of Chemistry and Mineralogy
University of Leipzig
Linnéstrasse 3, 04193 Leipzig (Germany)

Dr. H. J. Risselada
Department of Theoretical Physics
Georg-August-University
Friedrich-Hund-Platz 1, 37077 Göttingen (Germany)

Supporting information for this article can be found under: http://dx.doi.org/10.1002/anie.201605151.

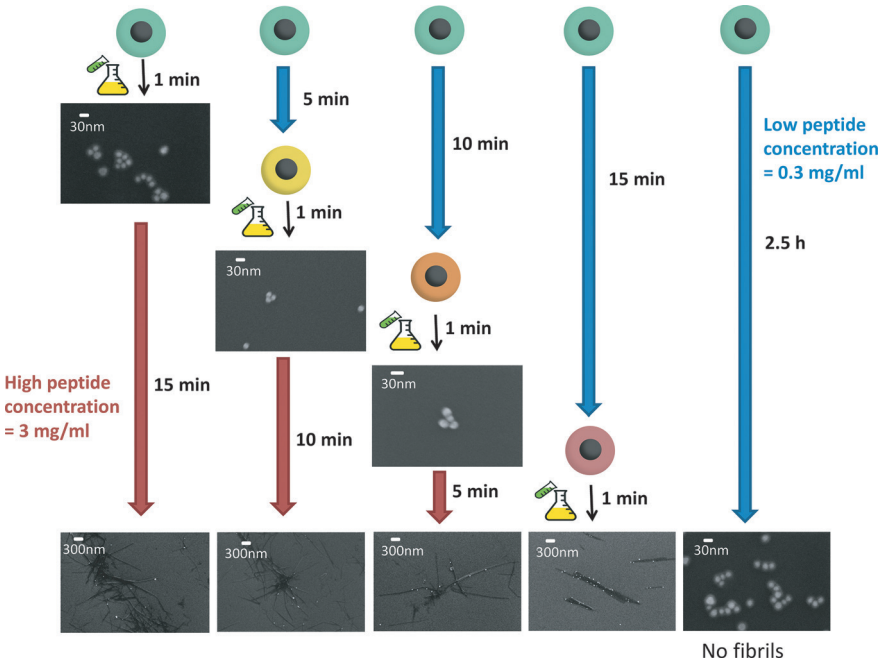

Figure 1. Experimental separation of the peptide organization effects in the vicinity of the NP surface from peptide–peptide interactions leading to rapid fibril growth. The initially low peptide concentration was increased after various incubation times t_1 (blue arrows), and the time needed until fibrils were detectable, t_2, (red arrows) was determined. In all cases, fibril formation was observed after $t_1 + t_2 = 15$ min. Note that the scale bars differ. The high-magnification images confirm that no (proto)fibrils started growing from the NPs. The low-magnification images illustrate the elongated structure of the fibrils.

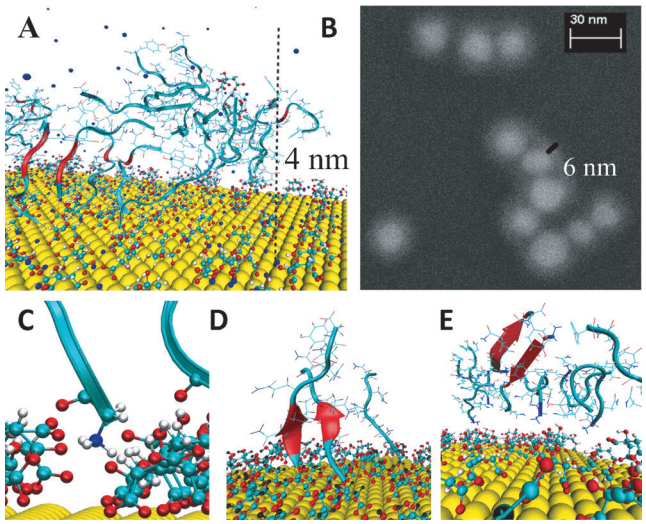

Figure 2. Adsorption of GNNQQNY peptides on a citrate-covered gold layer. A) Dimension of the peptide oligomers perpendicular to the gold plane as observed in MD simulations. B) Peptide halo around citrate-covered gold NPs, measured by scanning electron microscopy (SEM). C) N-terminus binding to oxygen anions of citrate. D) Three peptides "stand" on the surface, with the N-terminus (blue) bound to the citrate anions and the C-terminus extending into the solution. Two of them form a parallel dimer. E) Formation of a dimer with antiparallel β-sheet structure in the second adsorption layer of an adsorbed peptide cluster.

Herein, we will present a molecular mechanism of how surface interactions influence the growth of amyloid fibrils that is based on large-scale atomistic molecular dynamics simulations. The system consists of an explicitly solvated citrate-covered gold surface[8] with isotonic NaCl concentration and varying numbers of peptides (for technical details, see the Supporting Information). Both peptide species (the sequences from hIAPP and SUP35) adsorbed either directly onto the citrate-stabilized gold surface or onto other surface-bound peptides within the time scale of the simulation (100 ns). This initial adsorption of peptides onto the peptide-free surface is facilitated by Coulomb interactions between the positively charged N-terminus and the oxygen anions of the citrate molecules (Figure 2). However, once multiple peptides have adhered to the surface, this molecular picture changes as now a competition between peptide–peptide interactions and peptide–surface interactions is predominantly observed. When about 10% of the surface is covered with peptides, only few of the newly adhered peptides bind directly to the surface while most of them bind to already bound peptides. Accordingly, very fast oligomer formation is observed. These have an extension of about 2.5 nm to 4.5 nm perpendicular to the gold layer. This is in good agreement with the experimentally measured corona thickness of 4 nm to 7 nm (Figure 2 A and B).

Although our simulations both reproduce and explain the experimentally observed formation of peptide coronas around the NPs, it is not yet clear why fibril formation is accelerated and what happens within the 15 min that are needed to restructure the halo in a way that it becomes an efficient seed for fibril formation.

First, we considered the possibility that acceleration involves a collapse of the colloidal NP suspension, in which the stabilizing citrate molecules are outcompeted by adsorbed peptides. This hypothesis was excluded for three reasons (see the Supporting Information): 1) SEM images show that the NPs do not agglomerate significantly, but are rather present as individual particles (or in small groups of few particles) that are either adsorbed onto the fibrils or found within larger peptide aggregates (see Figure S13); 2) the zeta potentials of pure citrate-covered NPs and the peptide-coated colloidal NPs are essentially equal; and 3) the bare gold surface and the citrate-covered surface affect the behavior of adhered peptides in similar ways (see below).

Therefore, we hypothesized that the halo serves as a structural template that facilitates subsequent, orthogonal peptide stacking. The underlying mechanism is evidently linked to the slow formation of essential nucleation seeds, that is, critical oligomers, within the 4 nm to 7 nm thick halo.

To better mimic such a scenario, we additionally studied the behavior of a multitude of preformed oligomers near 1) the citrate-covered gold surface and 2) a surface that is densely packed with N-terminally bound peptides. We found that interaction with either the citrate-covered gold surface or the peptide monolayer led to complete dissociation of small, loose oligomers (dimers, trimers; Figure S6) whereas larger oligomers (linear hexamers, steric zipper octamers, and dodecamers) kept their original structure (Figure 3A and B). Oligomers formed out of N-terminally bound peptides within the (first) peptide monolayer necessarily consist of peptides that are oriented in parallel with respect to each other (Figures 2D and 3A). This explains why smaller, loose, antiparallel oligomers (dimers and trimers)[9] are relatively unstable when adhered on the citrate-covered gold surface while parallel dimers are spontaneously formed (Figure 2D). The electric field within the halo, however, does not prevent the formation of antiparallel dimers with peptides in the "second" layer in our simulations (Figure 2E). Therefore, we mainly attribute the destruction of loose oligomers by the densely packed peptide monolayer to competitive peptide–peptide interactions and only partly to the enforced alignment. Apparently, a predominantly unstructured monolayer does not provide a suitable scaffold for oligomers to grow into fibrils. Consequently, we stipulate that accelerated fibril growth requires the formation of structure already within the first peptide monolayer.

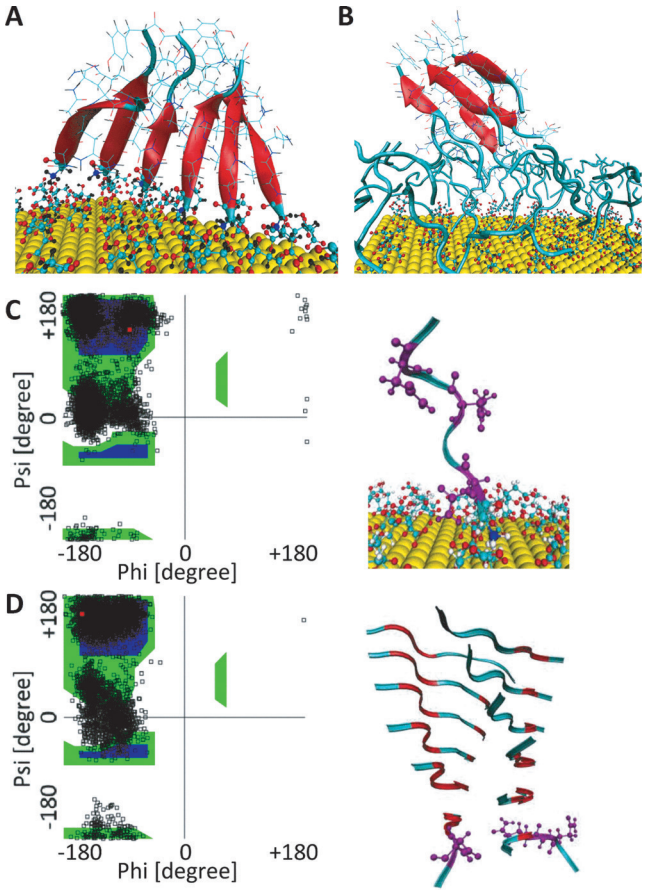

Figure 3. Ramachandran plots and typical structures. A) A preformed linear hexamer consisting of parallel β-strands aligning at the surface through N-terminal adsorption of the peptides. B) A preformed steric zipper hexamer (consisting of two β-sheets with three parallel peptide strands within each sheet and antiparallel orientation of the two sheets towards each other) assembles on top of the (preassembled) peptide halo in the second adsorption layer. C) A peptide monomer adsorbed on the surface (left) and the corresponding Ramachandran plot of ASN6 during the 100 ns trajectory (right). The Ramachandran plot is highly occupied at very low phi angles and psi angles around 0°. This unusual pattern was observed for all amino acids that are highlighted in purple (C, D right). D) A preformed steric zipper dodecamer and the corresponding Ramachandran plot of the highlighted amino acids (purple) at its growing end, here exemplified using GLN5 (right) during the 100 ns trajectory.

Nucleated crystal growth is largely controlled by translational and rotational entropy. The increase in peptide concentration near an attractive surface largely overcomes the barrier associated with translational entropy but does not necessarily overcome the barrier associated with rotational entropy. On the contrary, it may very well hinder the essential alignment of monomers and thereby oppose fibril growth. In contrast, the N-terminal physisorption to the surface that was observed in our study overcomes the rotational entropy barrier by properly aligning the peptides and reinforcing the growth of oligomers consisting of parallel β-strands. Earlier simulation works have demonstrated that GNNQQNY dimers assemble predominantly with antiparallel orientation,[9] whereas further monomers add mainly in parallel orientation, which is consistent with the crystal structures of the corresponding microcrystals published by Sawaya and coworkers.[10] Accordingly, in the "second" layer and in free solution, we observed initial β-sheets that are predominantly antiparallel, whereas the N-terminal alignment in the first monolayer directly leads to parallel oligomers. Therefore, we attribute the experimentally observed lag time to the relatively slow formation of regular, stable β-sheets near the surface of the NPs.[11]

Furthermore, our simulations illustrate that surface-bound peptides display a very distinct sampling of dihedral angle space (Ramachandran plot) with a very high probability for very low phi angles ($< -155°$) and psi angles around 0° (Figure 3C). These angles show a high degree of flexibility and frequently adopt regions in the phi–psi space that are characteristic for β-sheets. These states in the Ramachandran plot were also observed at the loose ends of different preformed oligomers with cross-β-sheet structures (Figure 3D and Figure S11). This observation suggests that the uncommon phi and psi states are occupied during the growth of amyloid fibrils by monomer addition at the ends of the fibril.[12] Fibril-compatible structures are thus formed on both the monomeric and the oligomeric level.

Finally, we explored how these mechanisms depend on the presence of adhered citrate molecules, which play a predominant role in the observed N-terminus–surface interactions. We thus repeated our simulation protocol with a bare gold surface (see Figure S7). Although the initial adsorption mechanism is different, the final outcome is very similar: The backbones of the peptides eventually rise up as a result of ongoing peptide–peptide and peptide–surface interactions. In GNNQQNY, the aromatic ring of tyrosine (Y) facilitates predominant C-terminal binding. The Ramachandran plots of

these peptides display a very similar pattern as illustrated in Figure 3C and D for citrate-bound peptides (see Figure S7). Accordingly, we conclude that the interactions of multiple peptides with a polarizable metal surface ultimately lead to similar structures as on a citrate-stabilized gold surface, which is consistent with earlier experimental studies with differently stabilized gold and silver NPs.[2]

Our model further shows that the competition between the underlying peptide–peptide and peptide–surface interactions must strike an essential balance to accelerate fibril growth.[4] If the peptide–surface interaction is too strong, restructuring of the initially adsorbed peptides does not take place, and fibril growth is slowed down or inhibited.[13] In case of a very weak peptide–surface interaction, the peptide–peptide interactions dominate and the NP surface hardly influences the system.[14] Only if both interactions compete, partial N- or C-terminal physisorption can occur, and the dihedral angle space of the peptide will resemble that of the ends of growing fibrils. Here, fine-tuned interactions between the NP surface and the terminal groups of the peptide, whether they rely on polarizability, charge, π stacking, or van der Waals interactions, seem essential to overcome the rotational entropy barrier and reinforce the formation of parallel, fibril-compatible oligomers. The need for well-balanced peptide–peptide and peptide–surface interactions confirms and extends the widely accepted hypothesis of a condensation–ordering mechanism.[4]

To further test this hypothesis, we experimentally investigated the influence of oxygen-terminated nanodiamonds (carboxyl and hydroxy groups) and polyethylene glycol (PEG) coated gold NPs (see Table S3).

The nanodiamonds have very similar properties to citrate-covered gold NPs. Namely, the zeta potential and the average size (gold NPs: $d \approx 20$ nm, $\zeta = -40 \pm 5$ mV; nanodiamonds: $d \approx 29$ nm, $\zeta = -40 \pm 5$ mV) are very similar. Therefore, we expect the same N-terminal binding mechanism for both NPs. However, the strength of the interaction is different. The polarizability of the gold surface induces a positive charge, which counteracts the negative surface charge of the citrate molecules. As the zeta potential is identical for both NPs, the negative charge density on the gold surface must therefore be larger (more carboxylic acid groups) than the corresponding surface charge density of the nanodiamonds. Thus we expected a weaker interaction with the N-termini of the peptides in case of the nanodiamonds and the peptide–peptide interaction to dominate.

In contrast, PEGylated gold NPs have the same polarizable gold core as citrate-stabilized gold NPs. However, the PEG layer leads to an increase in the zeta potential from -40 ± 5 mV to -23 ± 5 mV. Therefore, the attractive force between the positively charged N-termini of the peptides and the surface was expected to be weaker.

Accordingly, the accelerating and structure-inducing effects of the nanodiamonds and the PEGylated gold NPs should be small or even non-detectable. Our experiments indeed show that both NP species adsorb to the peptide aggregates, but have no significant influence on the kinetics or structure formation (see Figures S14 and S15). This finding supports the hypothesis that the balance between peptide–peptide and peptide–surface interactions is essential to accelerate fibrillation.

In conclusion, we have proposed a comprehensive and consistent mechanism for how (metallic) surfaces influence fibril formation for the amyloid-forming sequences of hIAPP and SUP35. Paradoxically, by accelerating the formation of large stable fibrils, NPs might prevent the formation of smaller, more toxic oligomeric species and thereby in fact positively affect the (initial) progress of amyloid-related diseases. Furthermore, our proposed mechanism—specific surface interactions stabilize characteristic reaction intermediates of fibril nucleation—could be useful to better understand and exploit the interaction of amyloid peptides with surfaces in general. It may shed light on how plasma membranes actively facilitate amyloid oligomerization or fibril growth, and why chemical modifications such as lipid peroxidation affect fibril formation. Furthermore, we may alternatively exploit and improve surface-based catalysis for the industrial fabrication of functional fibrils.

Acknowledgments

We thank G. Brancolini and S. Corni for insightful discussions, helpful hints, and especially for providing force field parameters for gold and citrate. Discussions of several important aspects of this work with F. Cichos, D. Huster, W. Jancke, and W. Paul are gratefully acknowledged. We thank the Deutsche Forschungsgemeinschaft for financial support through the SFB/TRR 102 and the state of Lower Saxony for support through the life@nano initiative.

Keywords: citrate-covered gold nanoparticles · hIAPP · molecular dynamics simulations · Ramachandran plots · SUP35

How to cite: *Angew. Chem. Int. Ed.* **2016**, *55*, 11242–11246
Angew. Chem. **2016**, *128*, 11408–11412

[1] a) S. Linse, C. Cabaleiro-Lago, W.-F. Xue, I. Lynch, S. Lindman, E. Thulin, S. E. Radford, K. A. Dawson, *Proc. Natl. Acad. Sci. USA* **2007**, *104*, 8691–8696; b) Y. Liao, Y. Chang, Y. Yoshiike, Y. Chang, Y. Chen, *Small* **2012**, *8*, 3631–3639.

[2] A. Gladytz, M. Wagner, T. Häupl, C. Elsner, B. Abel, *Part. Part. Syst. Charact.* **2015**, *32*, 573–582.

[3] a) T. R. Serio, A. G. Cashikar, A. S. Kowal, G. J. Sawicki, J. J. Moslehi, L. Serpell, M. F. Arnsdorf, S. L. Lindquist, *Science* **2000**, *289*, 1317–1321; b) J. Lee, E. K. Culyba, E. T. Powers, J. W. Kelly, *Nat. Chem. Biol.* **2011**, *7*, 602–609; c) A. Gladytz, E. Lugovoy, A. Charvat, T. Häupl, K. R. Siefermann, B. Abel, *Phys. Chem. Chem. Phys.* **2015**, *17*, 918–927.

[4] S. Auer, A. Trovato, M. Vendruscolo, *PLoS Comput. Biol.* **2009**, *5*, e1000458.

[5] M. Mahmoudi, I. Lynch, M. R. Ejtehadi, M. P. Monopoli, F. B. Bombelli, S. Laurent, *Chem. Rev.* **2011**, *111*, 5610–5637.

[6] M. Mahmoudi, H. R. Kalhor, S. Laurent, I. Lynch, *Nanoscale* **2013**, *5*, 2570–2588.

[7] a) S. Radic, T. P. Davis, P. C. Ke, F. Ding, *RSC Adv.* **2015**, *5*, 105489–105498; b) R. Vácha, S. Linse, M. Lund, *J. Am. Chem. Soc.* **2014**, *136*, 11776–11782.

[8] a) G. Brancolini, A. Corazza, M. Vuano, F. Fogolari, M. C. Mimmi, V. Bellotti, M. Stoppini, S. Corni, G. Esposito, *ACS Nano* **2015**, *9*, 2600–2613; b) G. Brancolini, L. Z. Polzi, S. Corni,

J. Self-Assem. Mol. Electron. **2015**, *2*, 1 – 26; c) F. Iori, R. Di Felice, E. Molinari, S. Corni, *J. Comput. Chem.* **2009**, *30*, 1465 – 1476; d) M. Hoefling, F. Iori, S. Corni, K.-E. Gottschalk, *Langmuir* **2010**, *26*, 8347 – 8351.

[9] Z. Zhang, H. Chen, H. Bai, L. Lai, *Biophys. J.* **2007**, *93*, 1484 – 1492.

[10] M. R. Sawaya, S. Sambashivan, R. Nelson, M. I. Ivanova, S. A. Sievers, M. I. Apostol, M. J. Thompson, M. Balbirnie, J. J. W. Wiltzius, H. T. McFarlane et al., *Nature* **2007**, *447*, 453 – 457.

[11] A. Morriss-Andrews, G. Bellesia, J.-E. Shea, *J. Chem. Phys.* **2012**, *137*, 145104.

[12] S. R. Collins, A. Douglass, R. D. Vale, J. S. Weissman, *PLoS Biol.* **2004**, *2*, 1582 – 1590.

[13] a) L. Xie, Y. Luo, D. Lin, W. Xi, X. Yang, G. Wei, *Nanoscale* **2014**, *6*, 9752 – 9762; b) J. Guo, J. Li, Y. Zhang, X. Jin, H. Liu, X. Yao, *PloS One* **2013**, *8*, e65579.

[14] A. Morriss-Andrews, G. Bellesia, J.-E. Shea, *J. Chem. Phys.* **2011**, *135*, 085102.

Received: May 26, 2016
Published online: August 11, 2016

